International Journal of Geospatial and Environmental Research

Volume 8
Number 2 *Geospatial Technology in Sustainable Cities and Communities*

Article 5

July 2021

Geological Lineament Assessment from Passive and Active Remote Sensing Imageries

Ainyyafiatty Arifin
Universiti Teknologi MARA, ainyyarifin@gmail.com

Nor A. Adnan
Universiti Teknologi MARA, adnannoraizam@gmail.com

Geological Lineament Assessment from Passive and Active Remote Sensing Imageries

Abstract

Lineament is any extensive linear feature on the Earth's surface that can be identified when there is a change in the topographical data. The advancement of technologies in remote sensing and Geographical Information Sciences (GIS) lead to the various studies and methods in mapping lineaments due to the availability of data from small to large scale areas. Lineament can be extracted from remote sensing data either with manual, semi-automatic or automatic image processing techniques that incorporate in numerous remote sensing and GIS software. Manually digitizing or tracing the aerial photograph is a subjective method as the lineament will be interpreted based on geomorphological understanding in determining the possible relationship between the linear features. Therefore, this research proposed automatic lineaments extraction techniques that less time-consuming compared to the semi-automatic and manual approaches as the algorithms for lineament detection have been integrated in the software. The aim of this study is to compare multi-sensors active and passive remote sensing technologies of Landsat 8, Sentinel 1 and Sentinel 2 satellite data in lineament mapping, based on automatic image processing tools between the state boundaries of Selangor and Pahang in Peninsular Malaysia. Overall, statistics descriptions, density, and orientations analysis indicate a correlation between the extracted lineaments and the geology of the area. Furthermore, lineaments extracted from Sentinel 1 radar images show the most significant result. Actually, the accuracy assessment of matching lineaments provides the Sentinel 1 as the best sensor compared to both the Sentinel 2 and the Landsat 8, with root mean square errors (RMSE) equal to 1.660, 1.743 and 2.757, respectively. Therefore, both remote sensing technologies and geographical information sciences can be effectively integrated within the field of structural geology, thus allowing the mapping of lineaments in a more practical, cost and time-effective way.

Keywords

geology, lineament, image satellite, sentinel, image processing

Acknowledgements

The authors wish to thank all the lecturers at the Centre of Studies Surveying Science and Geomatics, Faculty of Architecture Planning and Surveying, UiTM for comments and feedbacks for research output improvement.

1 INTRODUCTION

The term "lineament" was proposed by Hobbs (1904) to describe the spatial relationship between the landscape features. Then, in the study of the structural geology, O'Leary et al. (1976) redefined lineament as extended mappable linear or curvilinear structures signifying folds, fractures, or faults. The topographical data and geophysical analyses that reflect the rock's properties can be used to visually identify lineament (Tiren, 2010). Thus, any prominent linear features on the Earth's surface that reveal the rock basement's hidden architecture are referred to as lineament.

The geological lineaments have previously been mapped using traditional geological fieldwork mapping methods, in which geologists must personally go out to the field to observe exposures, outcrops, and landforms in order to determine the structural geology of an area. This method calls for excessive cost, time consuming and challenging. Due to the topography changes and lack of exposures, geologist often have difficulty mapping lineament structures such as strike-extensive faults during fieldwork (Yeomans, 2019). In addition, most of the remote areas are inaccessible for fieldwork and constrained to numerous scales that cause the data least updated in the last decade.

The early lineament mapping studies using remote sensing technologies began with the interpretation of aerial photos, and have evolved from unenhanced to digitally enhanced satellite images (Akhir, 2004). Then, the rigorous development of computing system offers automatic lineaments extraction techniques that much less time-ingesting compared to the manual and semi-automated methods as the algorithms for lineament detection has been integrated in the software. Preceding research in the discipline of the lineaments mapping highlighted that the automatic lineaments detection from satellite images is the most realistic method to provide lineament maps (Adiri et al., 2017; Farahbakhsh et al., 2020). However, the output will range in line with the employed satellite images because of the distinctive spatial and spectral resolution of the available sensors.

Considering that there are no specific studies about which satellite images produce the most constant output with respect to the map created from conventional mapping techniques, this presented study aims to assess the accuracy of lineament maps generated from the passive and active remote sensing data of Landsat 8, Sentinel 2 and Sentinel 1 sensors that undergo computerized or automatic lineament detection, by way of assuming as reference the published geological map. It is also designed to focus on the importance of GIS in geospatial analyst while analysing the geometry of the output data. This research will provide a valuable and persuasive guide for geologists and other possible users in determining lineaments without conducting field surveying in observing the physical geology of the study area. For instance, lineament maps can be utilised to find probable landslide areas and uncover sustainable groundwater resources (Mogaji et al., 2011 and Ramli et al., 2010). Thus, they can make use of the output to support sustainable developments while meeting the economic and social demands.

2 LITERATURE REVIEW

2.1 Lineament Mapping Using Remote Sensing Techniques

Lineament mapping in Malaysia has constantly developed during the last decade. Lineaments in the Upper Perak Valley were mapped with the Landsat Multispectral Scanner (MSS) in the early 2000s, while prior lineament mapping in Malaysia had relied on aerial photography and non-enhanced satellite images (Akhir, 2004). The study employs a variety of digital image processing techniques, including filtering to improve lineament visibility, and it has been proven that Landsat MSS pictures are extremely useful for structural (lineament) mapping and interpretation. Then, in a study by Yusof (2009), he demonstrates the usage of multispectral Landsat Thematic Mapper (TM) and Enhanced Thematic Mapper Plus (ETM+) satellite data to identify and interpret lineament in Malaysian tropical forest, and his results show that the manual extraction of remote sensing method is capable of extracting lineament trends in the tropical forest that are inaccessible by traditional survey methods. The Landsat TM image was also used to map the lineaments of the eastern part of the Gua Musang, in Kelantan to Cameron Highland Road, in Pahang with directional filtering and manual tracing techniques (Hashim, 2010) based on visual interpretation. According to the findings, the Landsat TM image with a single band photograph is the best source for mapping the lineament, particularly to the employment of directional filtering technique in image processing phase.

As stated in Ramli et al. (2009), the shaded relief derived from the Digital Elevation Model (DEM) is useful in locating faults and lineaments and has been employed in their study to verify that only negative lineaments are delineated for lineament mapping in a tropical environment. According to Abdullah et al. (2010), shaded relief images generated from Digital Elevation Models (DEMs) are helpful in identifying lineaments in different distinct relief and topography because this approach can enhance lineaments at specific orientations by simulating topographic illumination under various light directions. The enhancement of lineaments within the four sun azimuth directions is obtained by combining four shaded relief images into a final image, and DEM-based hill shading has led to the finding of positive and negative lineaments in the studied area, which had not been discovered by means of other satellite data interpretation methods and may even resolve a range of problems in geomorphology and geology researches.

Then, based on their observations in mapping lineaments of the Semanggol Formation, Azman et al. (2018) concluded that the Landsat 8 may be utilised efficaciously to trace structural information (lineaments) from any area in Malaysia. They apply a variety of digital processing technique such as atmospheric correction, geometric correction and histogram equalization to cast off errors in the image. After that, pan-sharpening with band 8 was conducted using ENVI 5.3 software and various spectral bands and band combinations for lineament tracing based on visual evaluation were performed to increase the picture quality up to 15 m resolution.

According to a case study in the Alichur Area of SE Pamir, sentinel data provide a higher number of lineaments and better results in terms of structural lineament recognition accuracy than optical sensors by analysing the gained results, shaded relief, density maps, and rose diagrams of the extracted lineaments in comparison to the directional filter image and existing faults, as well as the field survey (Javhar et al., 2019). Thus, the spatial resolution of the imagery has a significant impact on the accuracy and quality of derived lineaments.

2.2 Lineament Extraction and Analysis

In the previous work, many approaches were used to detect and analyse linear features from remote sensing data. The directional and non-directional filtered pictures, as well as the contrast stretched image of TM band 4, were employed in a study by Akhir and Abdullah (2009). Following the tracing of all lineaments, the orientations and lengths of each were identified and measured, and the data was evaluated using rose diagrams for interpretation and comparison with the published geological map. Aside from the rose diagram, a lineament density map should be created to analyse the lineament retrieved. According to Sarkar and Kanungo (2004), the density analysis used the kernel density adapted from the quadratic kernel function will classify the output into three categories: low, moderate, and high-density areas. Yusof et al. (2011) mention that the summed length of lineaments with a specified unit area of the grid is known as length density, while the number of lineaments per unit area or in each pixel is known as number of lineaments, and the number of intersection points at a specific per unit area is known as intersection of lineament density. Then, according to a study by Han et al. (2018), density analysis is a useful statistical analytic approach for investigating the spatial density distribution properties of lineaments and may provide clues to hidden structures and information on deep structures and mineralization where a high-density anomaly area generally denotes a fault or fold development area, whereas a low-density anomaly area represents a relatively stable tectonic.

Thus, the lineament map created from a satellite images should be examined for density, orientation, length, and association with a geological map. The extracted lineaments may be validated using GIS overlay techniques, as well as conducting spatial correlation and statistical analysis between the buffered distance from the lineaments and density per square kilometre with the historical geologic hazards in the study area (Elmahdy and Mohamed, 2016). Therefore, both GIS overlay and buffering may be utilised to evaluate the created lineament map, allowing the matching segments of the lineaments to be discovered and compared to the existing geological map for validity.

Lineament can be extracted using semi-automated or automated extraction procedures in addition to manual extraction techniques. Semi-automated mapping associated with algorithms for image enhancement steps such as transform or filter such as Principal Component Analysis, Laplacian, and Sobel filters (Yeomans et al., 2019). Al-Nahmi et al. (2016) used a semi-automated approach to develop a method for extracting and mapping lineament from Landsat 8 OLI in Yemen using several processing approaches such as Minimum Noise Fraction (MNF) bands (4,5,6), Color composites (7,5,3), PCA Principal Component Analysis bands (4,5,7), band ratios (7/5,6/4,4/2), directional filters, and image processing. Their findings are correlated with the geological situation of the observe area according to a report of the Geological Survey and Mineral Resources board of Yemen.

Based on a study in Sidi Flah-Bouskour inlier, Moroccan Anti Atlas that compares Advanced Spaceborne Thermal Emission and Reflection Radiometer (ASTER), Landsat-8, and Sentinel 1 data sensors in automatic lineament extraction, Adiri et al. (2017) claim that automated processes have become more requested than manual processes, which may be difficult, time-consuming, and highly dependent on the quality of the analysis. The evaluation of the collected results, which included a pre-existing geological map, lithological units, elevation data (slope, shading), density, orientation in relation to pre-existing faults, and a field survey, revealed that the Sentinel-1 outperforms optical sensors.

A novel geological lineament extraction technique based on a DEM and complemented by remote sensing imagery has been developed (Han et al., 2018). First, principal component analysis was used to determine the best independent band combination of Landsat 8 OLI images for lineament extraction. Second, the edges in the DEM and the composite Landsat 8 OLI images were sharpened using a high-pass Gaussian filter, and linear boundaries were identified using sensor based on the conspicuousness of the vector sum superposition features of the edge points. Finally, a Hough Transform (HT) was applied to search the edges and extract the geological lineaments. The results show that the proposed algorithm, which incorporates lineaments from the DEM and remote sensing images, can accurately reflect the direction and trend of geo-tectonic movements and agrees with regional geology and geomorphology, despite the fact that the length of the lineaments on the detection point tended to be shorter and defects arose when connecting them with the longer lineaments.

A study of the structural lineaments with automatic extraction from ASTER and WorldView-3 principal component orthogonal bands using the PCI Geomatica LINE Module algorithm has been performed by Chinkaka (2019). To extract the lineaments, the LINE Module algorithm parameter adjustment system used the field-based faults on the published geological map as a reference and the spatial pattern, orientation, length, and frequency of lineaments extracted from ASTER and WorldView-3 optical remote sensing data were compared to see how distinct these datasets are in mapping structural lineaments. Following the edge detection steps, the automated lineament extraction with the PCI Geomatica software's LINE module is performed as the Canny filter edge detection algorithm has been shown to outperform other edge detection operators in trials, and it is well-known as a reliable automatic edge detection method (Javhar et al., 2019).

Farahbakhsh et al. (2020) developed a framework for extracting geological lineaments using computer vision techniques. It is a combination of edge detection and line extraction algorithms for extracting geological lineaments using optical remote sensing data. The results show that using a minimum noise fraction transformation and a Laplacian filter, they were able to achieve a fine correlation between their extracted geological lineaments and the GSWA geological lineament map.

Those previous studies show that lineament mapping with remote sensing is becoming more prominent, and that various lineament extraction techniques can be adapted to produce better results in extracting lineaments, as well as emphasising the importance of GIS in analysing the extracted lineaments' output. Thus, the former methodology and techniques from the reviewed literature will be incorporated to accomplish this study for detecting and analysing lineaments extracted from multi-sensors data.

3 DATA AND METHODS

3.1 Study Area

The study area is located between Pahang and Kuala Lumpur, extends approximately for 800 km^2 (Figure 1) and it covers several mountainous peaks along the Titiwangsa Range, which naturally divides the east and west coast of the Peninsular Malaysia. The regional geology of the study area is generally made up from sedimentary and metamorphic rocks with alluvium or consolidated deposits. Lithology that associated with the study area are acid intrusive, schist, acid to intermediate volcanic, phyllite, slate, and limestones. The Bukit Tinggi Fault and the Kuala Lumpur Fault, both running northwest to southeast (NW-SE) and associated to the movements of the Indo-Eurasia plates, are two prominent geological fault lines in the area of interest (Abdul Latiff and Khalil, 2016). This area is ideal for lineament mapping since the fault lines are linked to the occurrence of earthquakes and geohazard phenomena (Lat and Ibrahim, 2009).

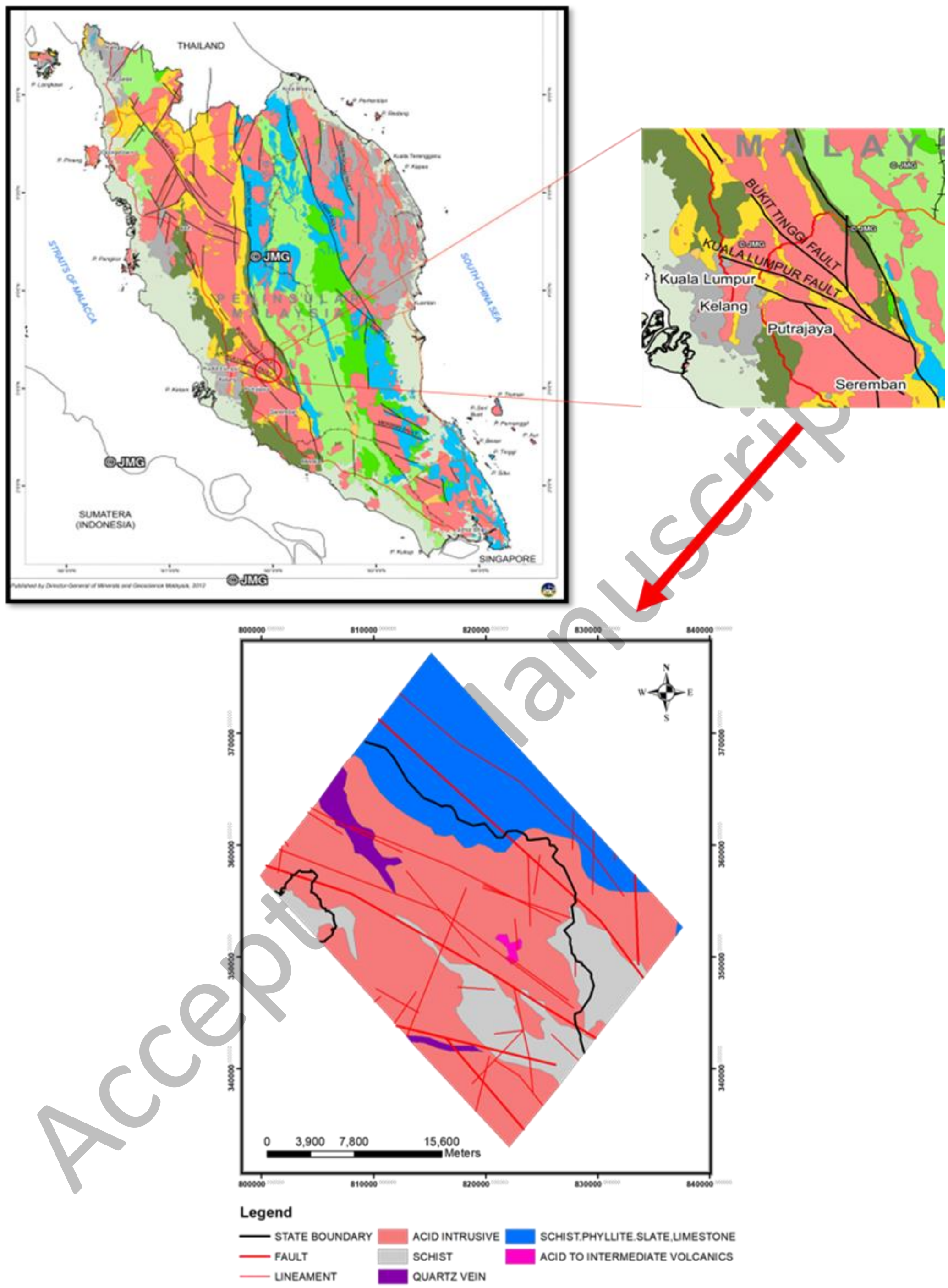

Figure 1. Geological setting of the study area that includes two major geological fault line that passed through the Peninsular Malaysia (JMG,2012).

3.2 Data and Processing

This study requires four main data sets including satellite images of Landsat 8, Sentinel 1 and Sentinel 2 as well as the Geological Map of the Peninsular Malaysia. Landsat 8 OLI and Sentinel 2 passive remote sensing data were obtained from the United States Geological Survey (USGS) website, while Sentinel 1 Synthetic Aperture Radar (SAR) active remote sensing data was obtained from the European Space Agency (ESA).

Landsat 8 carry Operational Land Imager (OLI) as sensor that operate with Thermal Infrared Sensor (TIRS). Landsat use optical sensors of passive remote sensing systems that measure the reflected sunlight at the sensor from sun as the source of energy to illuminate the surface and generate useful multispectral images during the daytime. OLI provide data that consist of eight bands of 30 m resolution and a panchromatic band of 15 m resolution. The panchromatic band will be utilised in this study as it has the highest spatial resolution that suitable to be used in examining large scale map area. Sentinel 2 also uses optical sensors, comparable to Landsat 8, to provide multispectral images by measuring visible to shortwave infrared (SWIR) wavelengths. Sentinel 2 consist of 13 spectral bands with spatial resolution from 60 m to 10 m. The highest spatial resolution band of Sentinel 2 data will be employed in the lineament extraction process.

Sentinel 1 is the first satellite mission of the Copernicus Program conducted by European Space Agency (ESA). It consists of two radar imaging satellites, Sentinel 1A and Sentinel 1B, which were launched in 2014 and 2015, respectively, with similar orbital planes of sun-synchronous orbit at 693 km altitude and 98.18° inclination. Sentinel 1 satellites are equipped with C-band synthetic aperture radar (SAR) instruments that transmit energy in the C-band of microwave regions at a frequency of 5.405 GHz, allowing for high-resolution imagery at any time of day or night and in any weather. SAR is an airborne-based geospatial data collection methods that known as active microwave remote sensing system as the sensor provides its own source of energy to illuminate the Earth's surface, emits microwave radiation to the surface and receives the reflected signal.

The multispectral images from Landsat 8 and Sentinel 2 sensors go through image pre-processing stages via directional filtering, histogram equalisation and principal component analysis (PCA), within the ERDAS IMAGINE™ software. Image enhancement techniques such as directional filtering can sharpen the border between adjacent units, while histogram equalisation modifies image intensities to improve pixel contrast and PCA removes redundant data to make it more apparent for interpretation (Thannoum et al., 2013; Marghany and Hashim, 2014; Estornnell et al., 2013). Meanwhile, Sentinel 1 data was solely calibrated in Sentinel Application Platform (SNAP) without passing through image enhancing phases in ERDAS due to the enormous documents sizes that are unsupported by ERDAS IMAGINE™.

The satellite data were then employed for automatic lineament extraction by means of the LINE Algorithm of the PCI Geomatica™ package. LINE is a PCI Geomatica feature that enables to extract linear features from an image and also save them as polylines in a vector layer (PCI Geomatics, 2019). The edge detection, thresholding, and curve extraction steps of the technique are used to calculate LINE. LINE is computed with three stages of the algorithm for edge detection, thresholding, and curve extraction.

The lineament will be identified automatically after the values for each parameter has been specified. The extracted lineament should be saved in vector format as a .shp file and loaded into ArcGIS. The extracted lineament's outputs were then examined and assessed using the ArcGIS™ toolbox's spatial analyst toolsets to portray the lineament's number, length, density, and orientations (Figure 2).

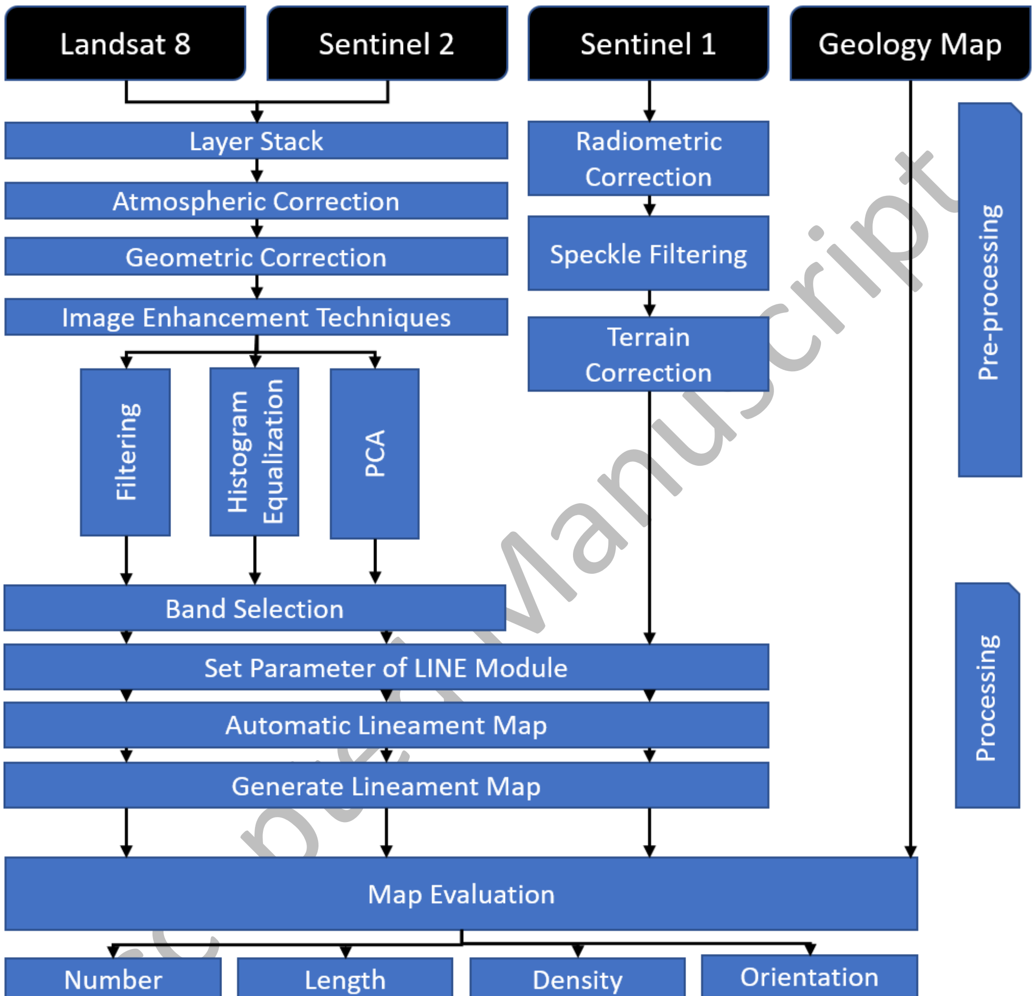

Figure 2. General workflow in data pre-processing, processing and post processing.

Spatial overlay techniques and buffering were applied to investigate the relation of the extracted lineaments with the structural geology of the study area with reference to the existing geological map. Root Mean Square Error (RMSE) then been calculated based on the matching and non-matching area of extracted lineaments that tolerate with the buffer regions.

Overlay analysis will be performed to combine the layers and integrate the spatial information with the attribute data. As the lineaments exist in vector as line features, vector overlay analysis that involve intersect, merge and union tools will be applied to display the relationship of lineament extracted automatically with the existing geological map. Then, buffer tool will be computed to test the lineament map with fault lines in the geological map. Buffer zone of 150 m will be assigned to find the matching lineaments with the faults as buffer regions of 150 m correspond to 10 pixels of 15 m resolution for panchromatic band of Landsat 8 and 15 pixels for 10 m spatial resolution of band 8 layer in Sentinel 2 data. As a consequence, there may be regions with non-matching and matching lineaments to the existing fault line.

By referring to 10 samples of lineament that match the lineament from the buffering output, the RMSE of the extracted lineament will be determined. The RMSE value reflects a quantitative study which indicates that extracted lineaments remain coherent with the lineaments represented on the geological map.

4 RESULTS AND DISCUSSIONS

4.1 Lineament Extraction Results

The main results for this study are the lineament map extracted from these multi sensors data (Figure 4). The relationship between the extracted lineaments and the available geological map is shown by qualitative and quantitative data analysis of the number, length, density, and orientations of extracted lineaments. Table 1 lists the quantitative values of the extracted lineaments' geometries as well as the RMSE for each sensor whereas Table 2 shows the statistics of linear features in the geological map that related to the research area.

Table 1. Quantitative results of the extracted lineaments from the different tested sensors.

	Landsat 8	Sentinel 1	Sentinel 2
Number of Lineaments	1608	6396	2637
Total Length (km)	687.841	2465.930	1045.929
Minimum Length (km)	0.03	0.222	0.300
Maximum Length (km)	3.229	2.088	1.417
Mean	0.428	0.386	2.626
Standard Deviation	0.254	0.174	0.104
RMSE	2.757	1.660	1.743

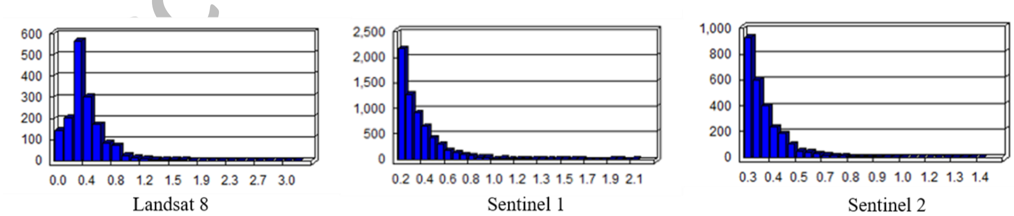

Figure 3. Frequency distributions of the lineaments extracted from Landsat 8, Sentinel 1, and Sentinel 2 respectively.

Table 2. Statistic of linear features in the existing geological map.

	Main fault line	Lineament
Number of Lines	5	33
Total Length (km)	100.231	203.502
Mean	20.044	6.166

Standard Deviation	10.918	7.183

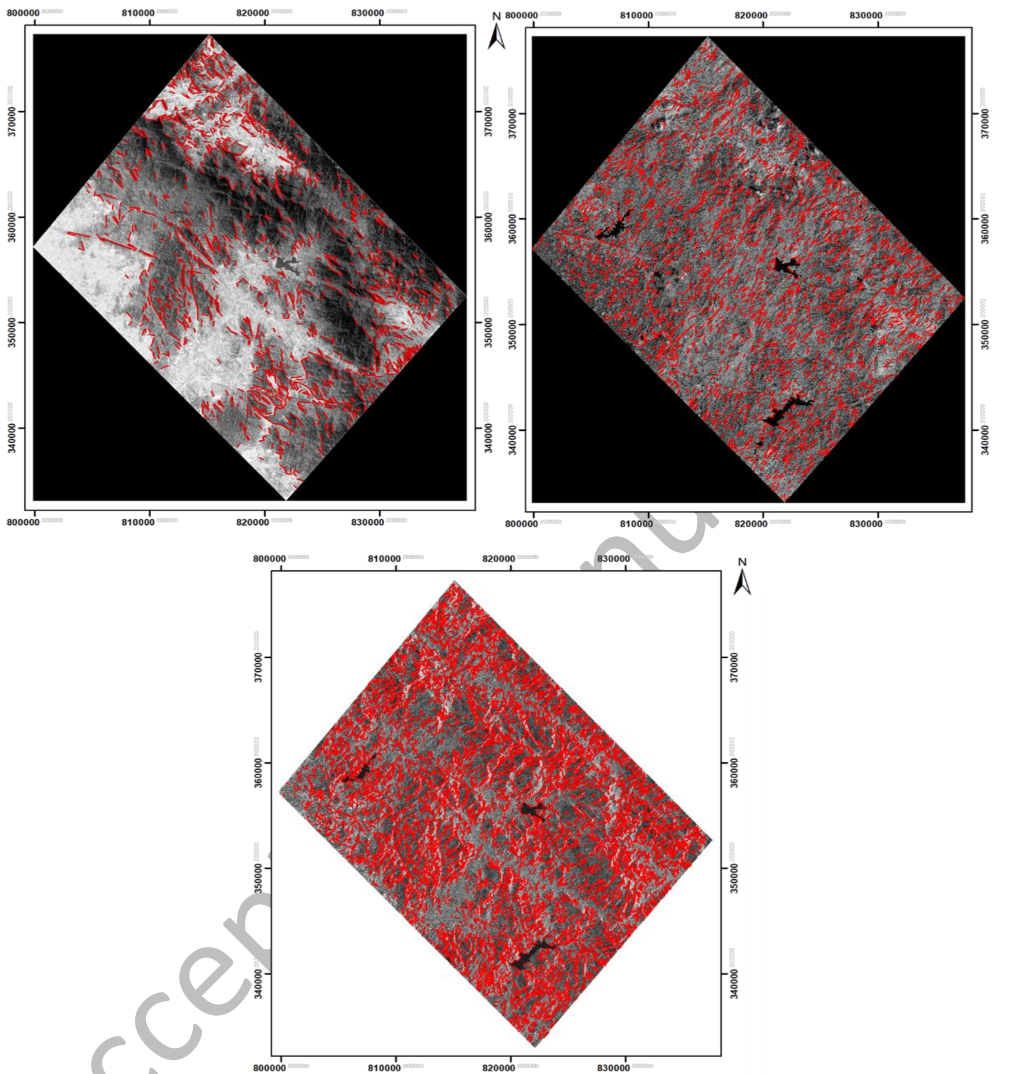

Figure 4. Lineament map extracted from Landsat 8 (top left), Sentinel 2 (top right) and Sentinel 1 (bottom) overlay with the satellite image of the study area.

According to Table 1 and frequency distribution (Figure 3), Sentinel 1 contains the most lineaments with 6810 counts, followed by Sentinel 2 with 2627 and Landsat 8 with 1608 counts that may be discovered using the automated extraction technique. The length of the extracted lineaments from these three different sensors shows mean values for length of the extracted lineament from Landsat 8, Sentinel 1, and Sentinel 2 in the range of 0.4 to 0.3, indicating that their length of lineaments is nearly identical, with only minor differences in elongation of the lineaments. In comparison to Sentinel 1 and Sentinel 2, Landsat 8 has the smallest minimum length lineaments. The greatest length of lineaments extracted from Landsat 8 are, however, longer than those retrieved from Sentinel 1 and Sentinel 2.

The distributions of the extracted lineaments were then examined using lineament density maps (Figure 5). Density analysis is a type of correlation analysis that is used to describe the frequency of lineaments per unit area in geological data. The green colour on the lineament density map shows a low frequency of lineaments per unit area, whereas the red region shows a site with more than 2.5 lines per square kilometre. Sentinel 1 has a high-density map area, with roughly 88 percent of the study area covered in red zone, but Sentinel 2 and Landsat 8 have just 20 percent and 16 percent of high-density map area, respectively. This is interrelated to the length and number of counts in the lineament map, as high occupancy of extracted lineaments increases lineament frequency per unit area. The majority of the high-density lineaments in Landsat 8 are concentrated in the north and south of the study area, but dense areas in Sentinel 2 are dispersed and high-density lineaments in Sentinel 1 cover the entire of the studied area.

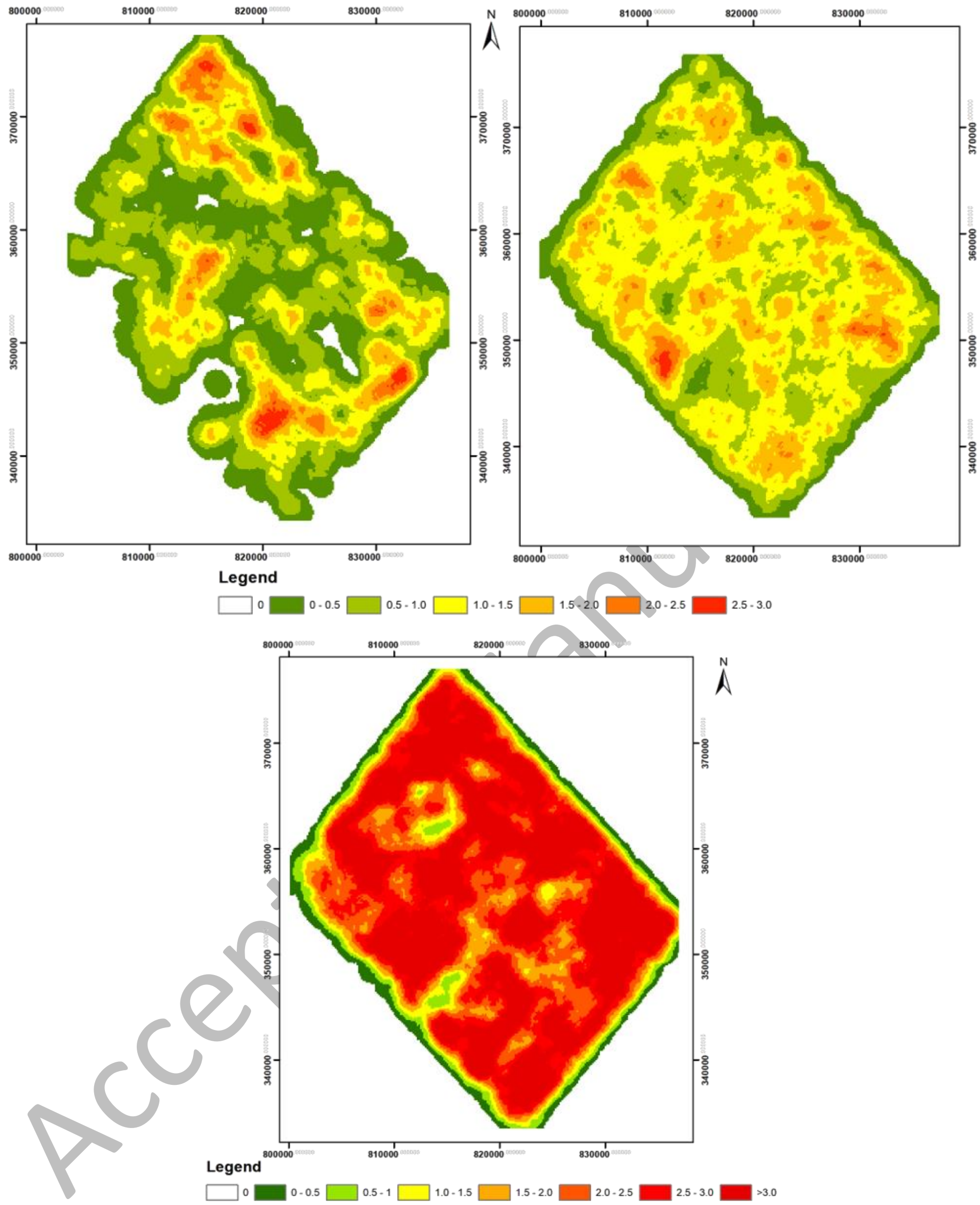

Figure 5. Lineament density maps of Landsat 8 (top left), Sentinel 2 (top right) and Sentinel 1 (bottom).

The extracted lineaments were displayed as a rose diagram to illustrate their orientations based on the end point of the coordinate indicating the trend of the structural features in the geological relation of the study area (Figure 6). Referring to the rose diagrams, most of the lineaments extracted from Landsat 8, Sentinel 1 and Sentinel 2 data are trending NW-SE, which is consistent with the orientation of the major fault lines of Bukit Tinggi Fault and Kuala Lumpur Fault as left-lateral or sinistral strike-slip faults (Figure 7) that trend NW-SE (Abd Manap et al., 2016).

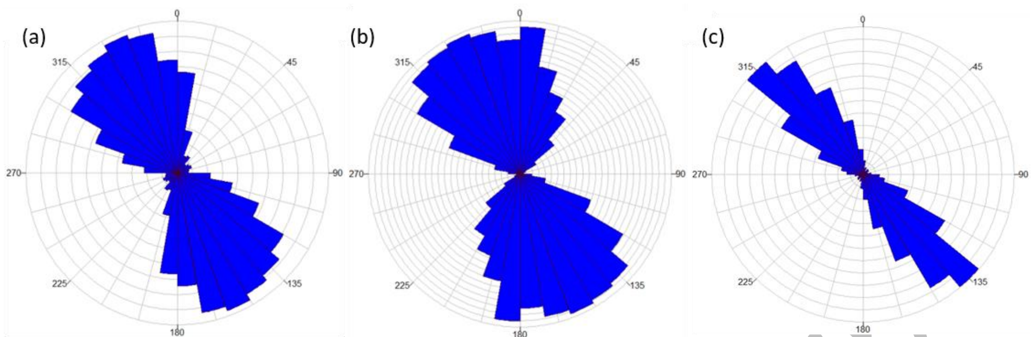

Figure 6. Rose diagrams of lineament extracted from Landsat 8 (a), Sentinel 1 (b), and Sentinel 2 (c) sensors, respectively.

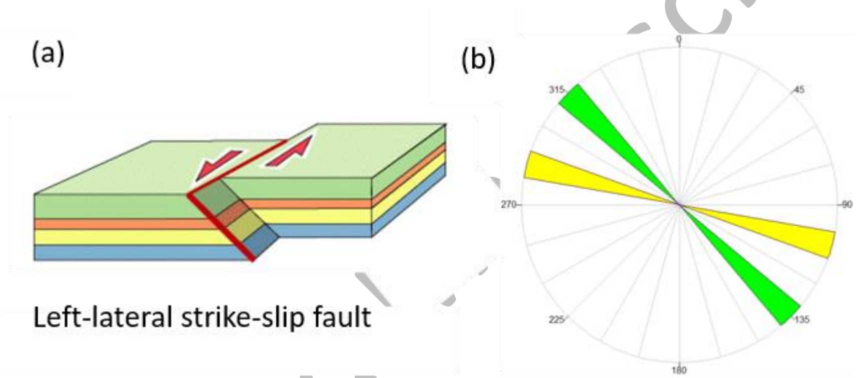

Figure 7. (a) Illustration of sinistral or left-lateral strike-slip fault where the left block moves toward and the right block moves away (Butler et al., 2009) and (b) Trending of Bukit Tinggi fault (green) and Kuala Lumpur fault (yellow) in a rose diagram.

4.2 Evaluation of Lineament Map

The generated lineament maps were compared to geological map by using GIS overlay techniques to reveal the data's relationship, pattern, and correlation (Figure 8,9, and 10). Query and further analysis can be performed based on the datasets of all layers. The relation between the trend of lineaments and the structural geology of the study area was inferred using proximity analysis with buffering. If the features are zoomed in to the buffered area, the intersection zone between the fault and extracted lineament lines can be observed (Figure 11).

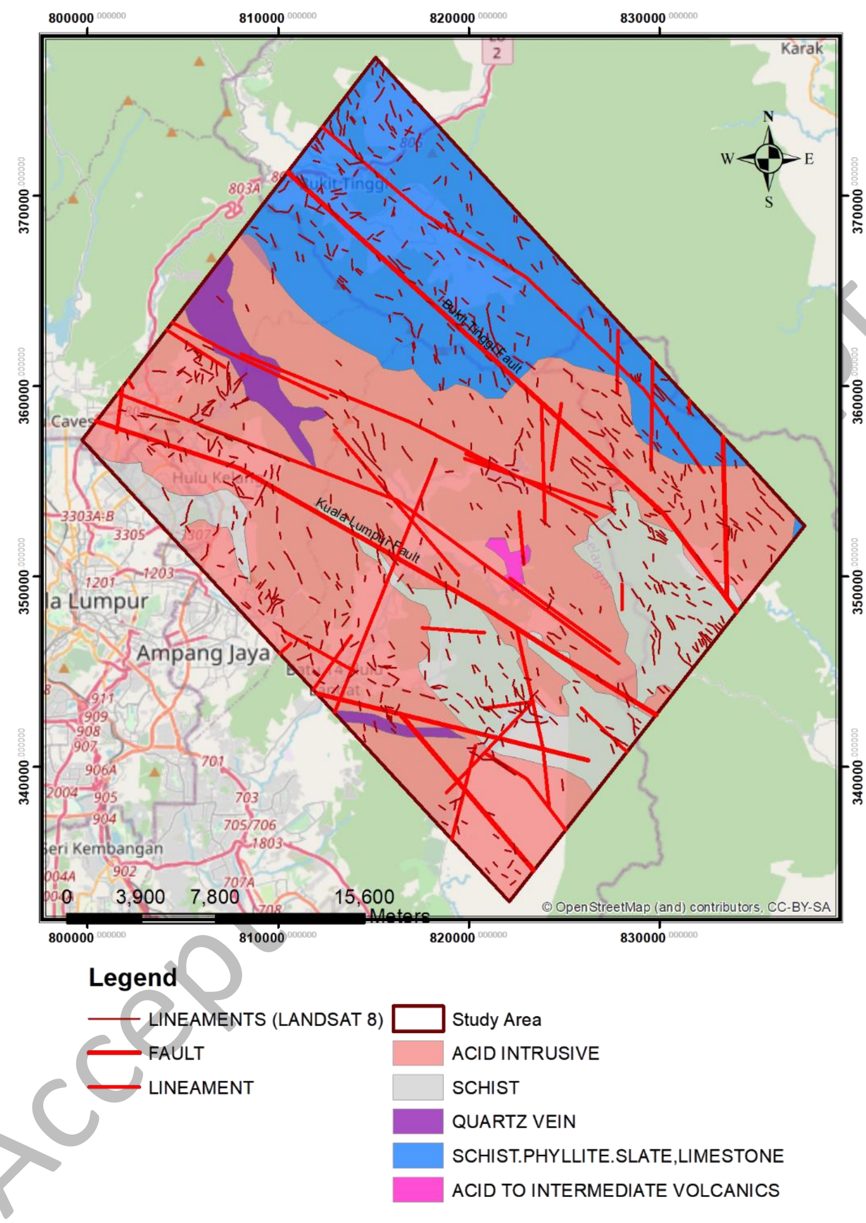

Figure 8. Overlay of the extracted lineaments from Landsat 8 to the geological map.

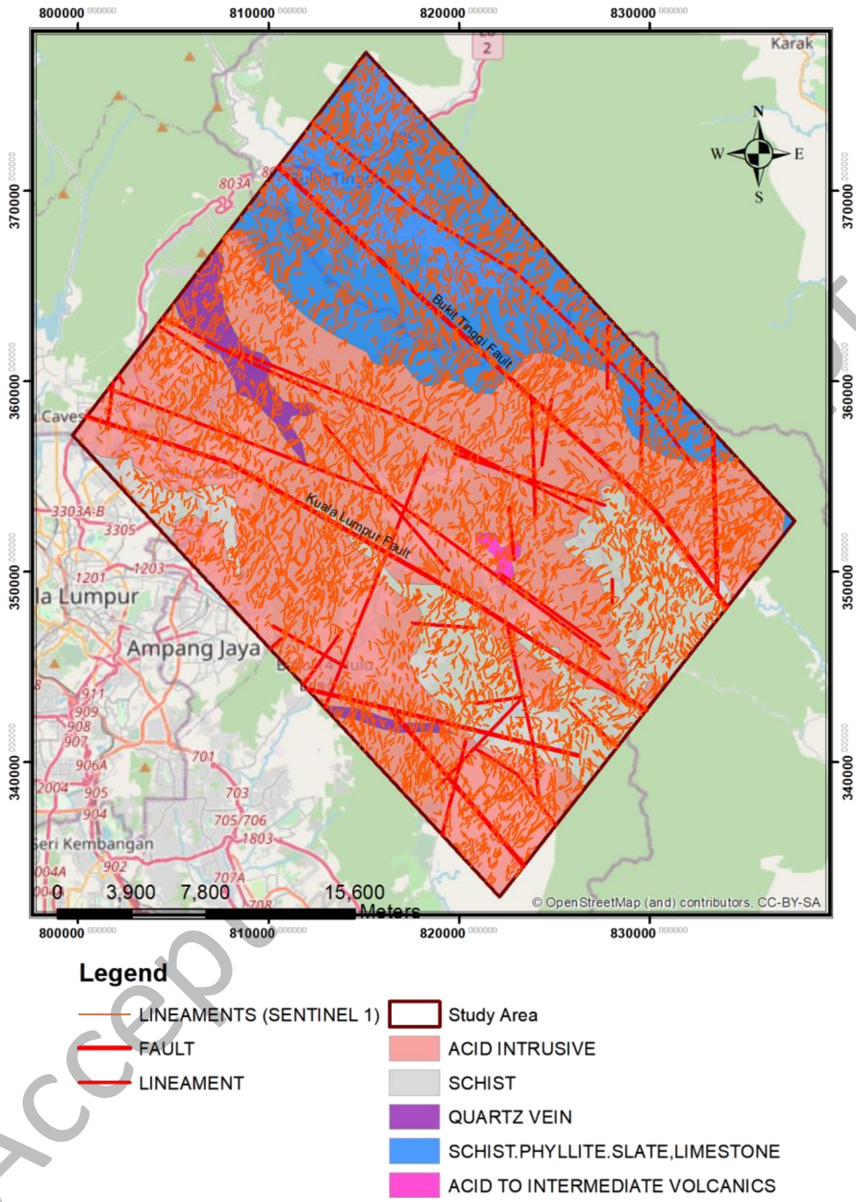

Figure 9. Overlay of the extracted lineaments from Sentinel 1 to the geological map.

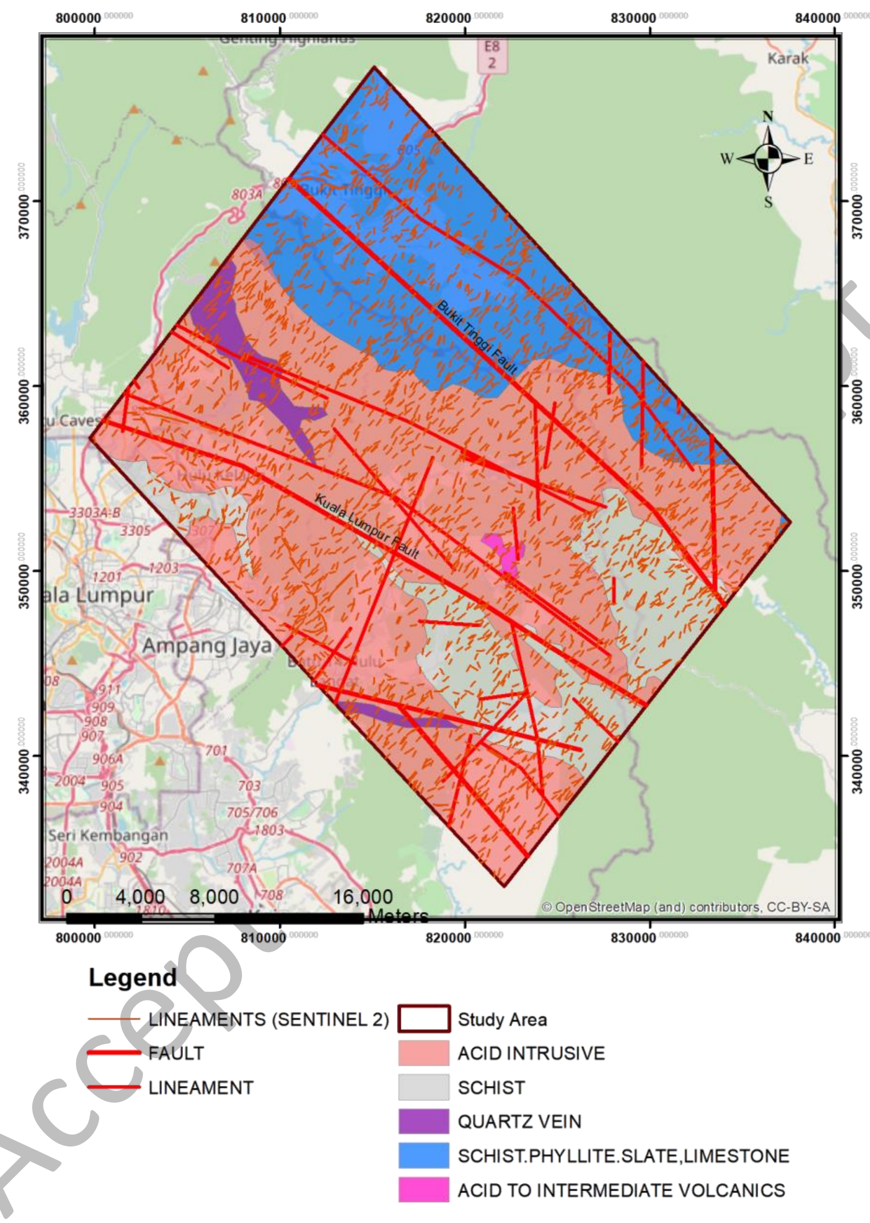

Figure 10. Overlay of the extracted lineaments from Sentinel 2 to the geological map.

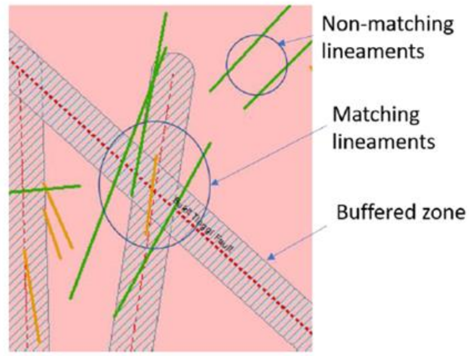

Figure 11. Example of matching and non-matching lineaments to the buffered zone

Matching and non-matching area of lineaments that tolerate with the buffer regions of 150 m that correspond to 10 pixels of 15 m resolution for the panchromatic band of Landsat 8 and 15 pixels for 10 m spatial resolution of band 8 layer in Sentinel 2 data were observed and used to calculate the RMSE as shown in Table 1. Figure 12 shows the example of matching and non-matching lineaments near the Bukit Tinggi Fault Zone and Kuala Lumpur Fault Zone respectively. Sentinel 1 appears to have the lowest RMSE of matching lineaments extracted, with a value of 1.66, which is 0.083 less than Sentinel 2 and 0.6 times less than the extracted lineament from Landsat 8.

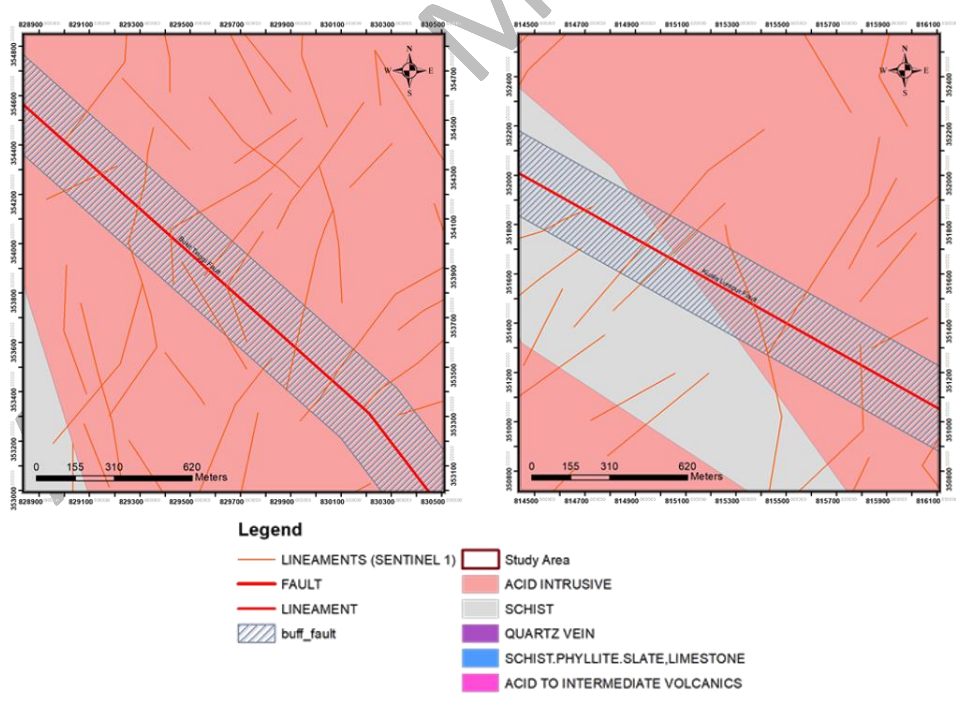

Figure 12. Example of matching and non-matching lineaments near Bukit Tinggi Fault Zone (left) and Kuala Lumpur Fault Zone (right)

4.3 Discussion

Based on the lineament map and statistical analysis, Sentinel 1 able to produce the highest number of lineaments extraction compared to the Sentinel 2 and Landsat 8. Referring to the pattern of lineaments in the geological map, most of the linear features are elongated and less likely to what can be seen from lineaments extracted in Landsat 8, Sentinel 1 and Sentinel 2. This might be linked to the spatial resolution of the Landsat 8 that make it less visible for the lineament to be automatically detected using LINE algorithm. Based on the data from Sentinel 1 and Sentinel2, radar images were shown to be more effective in detecting lineaments than multispectral images. The short lineaments most probably represent long linear features of lineaments in the study area. However, they tend to be disrupted and interrupted due to the visual representation of the images.

Sentinel 1 has more lineaments per unit area than Sentinel 2 and Landsat 8, according to the density analyses, since the number of lineaments in Sentinel 1 is greater than in Sentinel 2 and Landsat 8. This is correlated to the length and number of counts in the lineament map on purpose. When Sentinel 1 becomes occupied with a large number of lineaments, the density in the area tends to be higher than Sentinel 2 and Landsat 8, since the occupancy of large lineaments in Sentinel 1's large give hit in the intersection region.

The rose diagram in orientation analysis represents the tectonic process that trigger their creation. The trending of the orientations of lineaments indicates the direction of the structural geology of the area including strike, dip, azimuth, lineaments and fault orientations. Most of the lineaments extracted from Landsat 8, Sentinel 1 and Sentinel 2 are trending NW-SE that relatively similar to the major fault line of Bukit Tinggi Fault and Kuala Lumpur Fault.

Landsat 8, Sentinel 1, and Sentinel 2 can be employed for lineament studies based on statistical, density, and orientation analyses. In comparison to Sentinel 2 and Landsat 8, Sentinel 1 has significant linkages and correlations in terms of pattern, consistency, and orientations of the lineaments relative to the published geological map. Thus, Sentinel 1 radar data is more suitable and practical for automatic lineaments extraction methods compared to the optical image produces from passive remote sensing system in Landsat 8 and Sentinel 2.

Because most of the automatically generated lineaments correlate with the major fault line and follow the trend of the geological features on the map, the map evaluation using overlay and proximity analysis indicates that these satellite images may indeed be utilised to map the lineament. The automatically extracted lineaments might be inferred as geological linear features before being analysed for specific study purposes. According to the RMSE results, the lineament generated from Sentinel 1 has the least error, followed by Sentinel 2 and Landsat 8. As a result, lineament retrieved from Sentinel 1 produces the most coherent result with respect to the existing lineaments in the geological map.

5 CONCLUSION

The main purpose of this research is to evaluate different remote sensing approaches in lineament mapping using an automatic lineament extraction approach, which led to the discovery of GIS tools and remote sensing concepts. The findings of the study show that automated lineament extractions from active remote sensing data (Sentinel 1) outperform those from passive data (Landsat 8 and Sentinel 2). Sentinel 1 shows the best output when the percentage difference of the number of lineaments are 58.77% and 74.86 % higher than Sentinel 2 and Landsat 8 respectively. Furthermore, 88% of the region is covered by lines with a density of more than 2.5 lines per square kilometre, with a NW-SE trending that is significantly relative to the orientation of major fault line. The calculated RMSE also supporting Sentinel 1 as the most significant sensors for extracting lineament automatically with the accuracy assessment of 1.660 compared to 1.743 and 2.757.

Various technical problems might be encountered to conduct the automatic lineament extraction throughout the pre-processing, processing and post-processing techniques. The result of the automatic lineaments extraction is highly dependent on the image enhancement techniques to make sure the features of lineaments in the satellite images can be easily detected with the computed algorithms in the LINE MODULE within the PCI Geomatica Software. LINE algorithms should be taken into consideration as the six parameters in the algorithm can be customised based on the purpose of the study. The selected parameter that has been used in this study are based on the previous literature and several trials to match the data with the suggested parameters. It would be better if further study on the parameters uses in this algorithm be conducted to provide standard value relative to the various purposes of detecting linear features from different type of images.

Although the field survey is known as one of the best methods to produce the accurate results, the advance in the technology and development of geographical information sciences nowadays can assist the researchers, surveyors, and geoscientists in overcoming the limitations that they encountered during the fieldwork. With the existence of ranges satellite images that vary in spatial and spectral resolutions, its benefits users in utilizing the data based on their preference and decision-making skill. Thus, by knowing the pro and contra between the different sources and techniques in automatic lineament mapping might be beneficial to various field and industries that required preliminary study of lineaments before proceeding with their next works. This work is handy as most of the data are accessible and applicable for cost and time savings.

Apart of the remote sensing data, the gravitational, Light Detection and Ranging (LIDAR) and ground data can be integrated for further study in mapping the lineaments or the structural geology of an area. Seismic and geophysical data also precious for mapping the lineaments in the potential hydrocarbon resources area as well as predicting the geologic hazard of an area due to the presence of the linear features that relative to the tectonic movements in an area. Therefore, more studies that related to the lineament mapping that associated with the application of geographical information systems can be conducted to solve the real-world problem.

In conclusion, this study also believed to support the sustainable development goals set by the United Nation in making sustainable cities and communities that inclusive, safe, resilient and sustainable. This is relevant to the significant of lineament mapping in geohazards studies that include identification, assessment and mitigation of land geohazards. For instance, it is relevant to enhance landslide hazard assessment and slope stability analysis in reducing the adverse effects of natural disasters and environmental impact in the cities area. Thus, geographical information system and remote sensing technologies can be effectively integrated and employed in the field of lineaments mapping, especially for less accessible areas as well as contributing for innovative technologies and sustainable industrialisation.

REFERENCES

Abdul Latiff, A.H. and Khalil, A. E. (2016) Velocity Structure and Earthquake Relocations at Central Peninsular Malaysia Region Velocity Structure and Earthquake Relocations at Central Peninsular Malaysia Region. *Sixth International Conference on Geotechnique, Construction Materials and Environment,* 1–6. https://www.science-community.org/en/node/163996.

Abdullah, A., Akhir, J. and Abdullah, I. (2010) Automatic Mapping of Lineaments Using Shaded Relief Images Derived from Digital Elevation Model (DEMs) in the Maran – Sungi Lembing Area*. Electronic Journal of Geotechnical Engineering ,* 15, 949–957.
http://www.ejge.com/2010/Ppr10.066.pdf

Abd Manap, M., Shuib, M.K., and Ramli, M.F. (2016) Active Faults Mapping Using Remote Sensing and GIS Technique: A Case Study of Bukit Tinggi and Bentong-Karak Area, Malaysia. *37th Asian Conference on Remote Sensing.*
http://www.proceedings.com/33172.html

Adiri, Z., El Harti, A., Jellouli, A., Lhissou, R., Maacha, L., Azmi, M., Zouhair, M., & Bachaoui, E. M. (2017) Comparison of Landsat-8, ASTER and Sentinel 1 satellite remote sensing data in automatic lineaments extraction: A case study of Sidi Flah-Bouskour inlier, Moroccan Anti Atlas. *Advances in Space Research*, 60(11), 2355–2367.
https://www.sciencedirect.com/science/article/abs/pii/S0273117717306397

Akhir, J. (2004) Lineaments in enhanced remote sensing images : An example from the Upper Perak Valley , Perak Darul Ridwan. *Bulletin of the Geological Society Malaysia*, 48, 115–119.
https://gsmpubl.wordpress.com/2014/09/10/bulletin-of-the-geological-society-of-malaysia-volume-48-2004/

Akhir, J. M., & Abdullah, I. (2009) Geological applications of LANDSAT thematic mapper imagery : Mapping and analysis of lineaments in NW Penisula Malaysia. *Geospatialworld.net*, 1–8.
https://www.geospatialworld.net/article/geological-applications-of-landsat-thematic-mapper-imagery-mapping-and-analysis-of-lineaments-in-nw-penisula-malaysia/

Al-Nahmi, F., Alami, O. B., Baidder, L., Khanbari, K., Rhinane, H., & Hilali, A. (2016) Using remote sensing for lineament extraction in Al Maghrabah area - Hajjah, Yemen. *International Archives of the Photogrammetry, Remote Sensing and Spatial*

Information Sciences -42(21), 137–142. https://doi.org/10.5194/isprs-archives-XLII-2-W1-137-2016

Arenas-Abarca, M. A. (2006) Lineamennt Extraction from Digital Terrain Models: Case Study San Antonio del Sur Area , South-Eastern Cuba Lineament. *GeoInformation Science*, *March*, 80. https://biblioserver.sernageomin.cl/opac/DataFiles/11769v2pp11_14.pdf

Azman, A. I., Talib, J. A., & Sokiman, M. S. (2018) Lineament study of the semanggol formation and adjacent areas from landsat 8 image. *Bulletin of the Geological Society of Malaysia*, 65, 119–124. https://doi.org/10.7186/bgsm65201813

Butler, R., Casey, M., Lloyd, G., and McCaig, A. (2009). Web-based teaching resources in structural geology. *School of Earth Sciences, University of Leeds.* http://www.see.leeds.ac.uk/structure/learnstructure/

Chinkaka, E. (2019) Integrating Worldview-3 , Aster And Aeromagnetic Data For Lineament Structural Interpretation And Tectonic Evolution Of The Haib Area , Namibia Integrating Worldview-3 , Aster And Aeromagnetic Data For Lineament Structural Interpretation And Tectonic Evolution Of The Haib Area, Namibia. *Faculty of Geo-Information Science and Earth Observation of the University of Twente.* http://essay.utwente.nl/83441/1/chinkaka.pdf

El-Sawy, E.-S. K., Ibrahim, Atef, M., El-Bastawesy, M., & El-Saud, W. A. (2016) Automated, manual lineaments extraction and geospatial analysis for Cairo-Suez district (Northeastern Cairo-Egypt), using remote sensing and GIS. *International Journal of Innovative Science, Engineering & Technology*, *3*(5), 491–500. http://aucgeographica.cz/index.php/aucg/article/view/40

Elmahdy, S. I., & Mohamed, M. M. (2016) Mapping of tecto-lineaments and investigate their association with earthquakes in Egypt: a hybrid approach using remote sensing data. *Geomatics, Natural Hazards and Risk*, *7*(2), 600–619. https://doi.org/10.1080/19475705.2014.996612

Estornell, J., Martí-Gavliá, J. M., Sebastiá, M. T., & Mengual, J. (2013) Principal component analysis applied to remote sensing. *Modelling in Science Education and Learning*, *6*(7), 83. https://doi.org/10.4995/msel.2013.1905

Farahbakhsh, E., Chandra, R., Olierook, H. K. H., Scalzo, R., Clark, C., Reddy, S. M., & Dietmar, R. M. (2020) Computer vision-based framework for extracting geological lineaments from optical remote sensing data. *International Journal of Remote Sensing*, 41(5), 1760-1787.

Han, L., Liu, Z., Ning, Y., & Zhao, Z. (2018) Extraction and analysis of geological lineaments combining a DEM and remote sensing images from the northern Baoji loess area. *Advances in Space Research*, *62*(9), 2480–2493. https://doi.org/10.1016/j.asr.2018.07.030

Harris Geospatial Solutions. (2020) Sentinel-1 Intensity Analysis in ENVI SARscape Tutorial. *ENVI.* https://www.l3harrisgeospatial.com/docs/sentinel1intensityanalysistutorial.htm

Hashim, M,M. (2010) Lineament mapping using Landsat TM image in the eastern part of Gua Musang-Cameron Highland road. *Research and Development Seminar 2010, Malaysia.* https://inis.iaea.org/search/search.aspx?orig_q=RN:43035270

Hobbs, W.H. (1904) Lineaments of the Atlantic Border Region. *Geological Society Americal Bulletin*, 15, 483-506. https://pubs.geoscienceworld.org/gsa/gsabulletin/articleabstract/15/1/483/2468/Lineaments-of-the-Atlantic-Border-region

Javhar, A., Chen, X., Bao, A., Jamshed, A., Yunus, M., Jovid, A., & Latipa, T. (2019) Comparison of Multi-Resolution Optical Landsat-8 , Sentinel-2 and Radar Sentinel-1 Data for Automatic Lineament Extraction : A Case Study of Alichur Area , SE Pamir. *Remote Sens. 2019*, 11(7), 778. https://doi.org/10.3390/rs11070778

JMG. (2012), Geological Map of Peninsular Malaysia. *Department of Mineral and Geoscience Malaysia (JMG).* https://www.jmg.gov.my/en/awam/penerbitan/peta-gis-dalam-talian

Marghany, M., & Hashim, M. (2014) Lineament mapping using multispectral remote sensing satellite data. *International Journal of Physical Sciences,* 5(10), 1501-1507. https://doi.org/10.3923/rjasci.2010.126.130

Mogaji, K. A., Aboyeji, O. S., & Omosuyi, G. O. (2011) Mapping of lineaments for groundwater targeting in the basement complex region of Ondo State, Nigeria, using remote sensing and geographic information system (GIS) techniques. *International Journal of Water Resources and Environmental Engineering*, 3(7), 150–160. https://academicjournals.org/journal/IJWREE/article-full-text-pdf/57F993F54739

Mohammed, A., K, P., Kumanan, C. J., & Ramasamy, S. (2010) Significance of Surface Lineaments for Gas and Oil Exploration in Part of Sabatayn Basin-Yemen. *Journal of Geography and Geology*, *2*(1). https://doi.org/10.5539/jgg.v2n1p119

Muhammad, M. M., & Awdal, A. H. (2012) Automatic mapping of lineaments using shaded relief images derived from digital elevation model (DEM) in erbil-kurdistan, northeast Iraq. *Advances in Natural and Applied Sciences*, *6*(2), 138–146. http://www.aensiweb.com/old/anas/2012/138-146.pdf

Nugroho, H., Harris, R., Lestariya, A. W., & Maruf, B. (2009) Plate boundary reorganization in the active Banda Arc-continent collision: Insights from new GPS measurements. *Tectonophysics*, *479*(1–2), 52–65. https://doi.org/10.1016/j.tecto.2009.01.026

O'leary, D.W., Friedman, J.D., & Pohn, H.A. (1976) Lineament, linear, lineation:Some proposed new standards for old terms. *GSA Bulletin*, 87 (10), 1463–1469. https://doi.org/10.1130/0016-7606(1976)87<1463:LLLSPN>2.0.CO;2

Ramli, M. F., Tripathi, N. K., Yusof, N., Shafri, H. Z. M., & Rahman, Z. A. (2009) Lineament mapping in a tropical environment using Landsat imagery. *International Journal of Remote Sensing*, *30*(23), 6277–6300. https://doi.org/10.1080/01431160902842383

Sarkar, S., & Kanungo, D. P. (2004) An integrated approach for landslide susceptibility mapping using remote sensing and GIS. *Photogrammetric Engineering and Remote Sensing*, *70*(5), 617–625. https://doi.org/10.14358/PERS.70.5.617

Sarp, G. (2005) Lineament Analysis from satellite images, north west of Ankara.

Thannoun, R. G. (2013) Automatic Extraction and Geospatial Analysis of Lineaments and their Tectonic Significance in some areas of Northern Iraq using Remote

Sensing Techniques and GIS. *International Journal of Enhanced Research in Schience Technology and Engineering*, *2*(2), 1–11. https://doi.org/10.13140/RG.2.2.20851.99363

Tiren, Sven (2010) Lineament interpretation Short review and methodology. *Sweden.*

Yeomans, C. M., Middleton, M., Shail, R. K., Grebby, S., & Lusty, P. A. J. (2019). Integrated Object-Based Image Analysis for semi-automated geological lineament detection in southwest England. *Computers and Geosciences*, 123, 137–148. https://doi.org/10.1016/j.cageo.2018.11.005

Yusof, N. (2009). Lineament Mapping In Malaysian Tropical Forest Environment Utilizing Landsat Imagery. *Universiti Putra Malaysia.*

Yusof, N., Ramli, M., Pirasteh, S., and Shafri, H. (2011). Landslides and lineament mapping along the Simpang Pulai to Kg Raja highway, Malaysia. *International Journal of Remote Sensing.* 32(14), 4089-4105. http://dx.doi.org/10.1080/01431161.2010.484434